

## Conformations of Cyclic Octapeptides. 2. Crystal Structure of *cyclo*(D-Ala-Gly-Pro-D-Phe)<sub>2</sub>. Solvent Exposure of Backbone Protons in Crystal and Solution Conformations

Kenneth D. Kopple,\*† Gopinath Kartha,‡,± Krishna K. Bhandary,‡ and Krystyna Romanowska†

Contribution from the Department of Chemistry, Illinois Institute of Technology, Chicago, Illinois 60616, and the Roswell Park Memorial Institute, 666 Elm Street, Buffalo, New York 14263. Received November 30, 1984

**Abstract:** *cyclo*(D-Ala-Gly-L-Pro-D-Phe)<sub>2</sub> crystallizes from methanol-water in the monoclinic unit cell, space group *P*2<sub>1</sub>, dimensions  $a = 14.656 \text{ \AA}$ ,  $b = 12.585 \text{ \AA}$ ,  $c = 15.657 \text{ \AA}$ ,  $\beta = 134.07^\circ$ ,  $Z = 2$ . The asymmetric unit contains one peptide, one methanol, and two water molecules. X-ray crystallographic analysis reveals a peptide backbone conformation with approximate *C*<sub>2</sub> backbone symmetry containing only trans peptide bonds. The backbone in the crystal has type II  $\beta$ -turns at L-Pro-D-Phe, followed by type III turns at D-Phe-D-Ala. It differs from a solution conformation derived from NMR data primarily in an approximately 40° rotation of the plane of the Phe-Ala peptide bond relative to the local plane of  $\alpha$ -carbons. Solvent-accessible areas of peptide N-H protons were calculated for the crystal structure backbone and several conformations of the Phe side chain, and also for a backbone conformation more nearly approximating the proposed stable solution conformation. The calculated areas were compared with previously reported observed rate constants for *T*<sub>1</sub> relaxation of the N-H protons catalyzed by a nitroxyl radical, which is a proposed experimental measure of solvent exposure. The exposed areas calculated for the solution-like conformation more closely paralleled the observed nitroxyl rates than did those calculated for the crystal structure. Similar calculations were made for a model of the L-Ala-Gly-L-Pro-L-Phe-L-Ala unit of *cyclo*(L-Ala-Gly-L-Pro-L-Phe)<sub>2</sub>, which is thought to have in solution a stable backbone conformation that can be modeled by half of the backbone found in crystalline  $\beta$ -amanitin. In this case the crystal-derived surface areas were consistent with the nitroxyl data.

In a recent paper<sup>1</sup> four diastereomeric cyclic octapeptides, *cyclo*(D- or L-Ala-Gly-L-Pro-D- or L-Phe)<sub>2</sub>, prepared in a search for new classes of conformationally stable cyclic peptide backbones, were reported. Two of these, *cyclo*(D-Ala-Gly-L-Pro-D-Phe)<sub>2</sub> and *cyclo*(L-Ala-Gly-L-Pro-L-Phe)<sub>2</sub>, were judged by NMR criteria to have conformationally stable backbones, and conformations were proposed for them on the basis of NMR measurements of dimethyl sulfoxide solutions. In this paper we report a crystal structure of the D-Ala, D-Phe peptide and compare it with the proposed solution structure.

The backbone conformation reported here for the D-Ala, D-Phe peptide in the crystal differs slightly in one part of the molecule from a probable solution conformation. This difference is one that could affect the solvent exposure of backbone protons. Since the NMR data suggested it to be likely that only one backbone conformation is important in solution, it was instructive to calculate the accessible surface areas of the peptide backbone N-H protons of both the crystal structure and a model close to the proposed solution conformation. Such calculation of exposed areas have, for example, been described by Snyder<sup>2</sup> in a study of the conformations of the cyclic hexadepsipeptide roseotoxin B. In the present work, the calculated areas for the two models were compared with an experimental measure of solvent exposure, nitroxyl-catalyzed *T*<sub>1</sub> relaxation rates. A quantitative comparison of a calculated conformationally dependent variable with this measure of solvent exposure, which can only be made with conformationally stable molecules, has not been reported before. The comparisons confirm the existence of the suggested difference between crystal and solution conformations.

Similar calculations were also carried out for a model of the L-Ala, L-Phe cyclic octapeptide. The model used for this was derived from the crystal structure of  $\beta$ -amanitin,<sup>3</sup> to which the solution conformation of *cyclo*(L-Ala-Gly-L-Pro-L-Phe)<sub>2</sub> is considered to be closely related.<sup>1</sup> The exposed N-H surface areas calculated are consistent with the observed nitroxyl relaxation rate data.

### Experimental Procedures

**X-ray Analysis.** *cyclo*(D-Ala-Gly-L-Pro-D-Phe)<sub>2</sub> crystallizes from a solution in water-methanol to give well-formed crystals that are stable

outside the mother liquor. A crystal of dimensions 0.25 × 0.8 × 0.8 mm mounted on a glass fiber was used to determine cell constants and for intensity data collection. The octapeptide crystallizes in a monoclinic unit cell of dimensions  $a = 14.656 (2) \text{ \AA}$ ,  $b = 12.585 (1) \text{ \AA}$ ,  $c = 15.657 (2) \text{ \AA}$ ,  $\beta = 134.07 (2)^\circ$ , volume 2074.7  $\text{\AA}^3$ , space group *P*2<sub>1</sub>,  $Z = 2$ , and  $d_{\text{calcd}} = 1.237 \text{ g/cm}^3$ . Intensity data to  $2\theta = 154^\circ$  were measured on an Enraf-Nonius CAD-4 automatic diffractometer with Cu  $K\alpha$  ( $\lambda = 1.5418 \text{ \AA}$ ) radiation. During the course of data collection three reflections measured every 2 h showed no crystal deterioration. A total of 4577 unique reflections were measured, of which 4219 had intensities above  $2\sigma(I)$  and were used in structure solution and refinement. The intensity data were collected for Lorentz-polarization effects, and an empirical absorption correction was also made.

The structure was solved by using the direct methods program MULTAN 80.<sup>4</sup> With use of 371 reflections with  $E > 1.60$ , 130 phase sets were generated. An *E* map calculated by using the phase set with the highest combined figure of merit, 2.6221, revealed the positions of 32 atoms. The rest of the atoms were located from successive weighted Fourier maps. The asymmetric unit contains one octapeptide molecule, two water molecules, and one methanol molecule, a total of 58 non-hydrogen atoms. The structure was refined by full-matrix least squares, the atoms being treated isotropically in the initial stages of refinement. Toward the final stages of refinement anisotropic thermal parameters were used for all atoms except those of methanol. The final *R* factor for 4219 observed reflections was 0.081.

**Calculation of Accessible Areas of N-H Protons.** For *cyclo*(D-Ala-Gly-L-Pro-D-Phe)<sub>2</sub> the atomic coordinates of the crystal structure were used as input for the molecular surface program of Connolly.<sup>5</sup> The surface point density for these calculations was set at 60/ $\text{\AA}^2$ . Calculations were made for a probe radius of 0  $\text{\AA}$  (van der Waals surface) and 1.4  $\text{\AA}$ .<sup>2</sup> With use of the utilities of the CHEMLAB program package,<sup>6</sup> the Phe side chains were also rotated through  $\chi^1 = 60, 180$ , and  $-60^\circ$  and  $\chi^2 = 0$  and  $90^\circ$ . Pairs of these angles that gave bad contacts and high

(1) Kopple, K. D.; Parameswaran, K. N.; Yonan, J. P. *J. Am. Chem. Soc.* **1984**, *106*, 7212-7217.

(2) Snyder, J. *J. Am. Chem. Soc.* **1984**, *106*, 2393-2400.

(3) Kostansek, E. C.; Lipscomb, W. N.; Yocum, R. R.; Thiessen, W. E. *Biochemistry* **1978**, *17*, 3790-3795.

(4) Main, P.; Hull, S. E.; Lessinger, L.; Germain, G.; Declercq, J.-P.; Woolfson, M. M. MULTAN 80, 1980, a system of computer programs for the automatic solution of crystal structures from X-ray diffraction data, Universities of York and Louvain, 1980.

(5) Connolly, M. L. Molecular Surface Program, MS, program No. 429, Quantum Chemistry Program Exchange, Department of Chemistry, Indiana University, Bloomington, IN 47405, 1981.

(6) Pearlstein, R.; Malhotra, D.; Harr, R.; Hopfinger, A. J.; Potenzzone, R., Jr. CHEMLAB, Chemical Modeling Laboratory, 1981.

\* Illinois Institute of Technology.

† Roswell Park Memorial Institute.

‡ We regretfully record Dr. Kartha's decease, June 18, 1984.

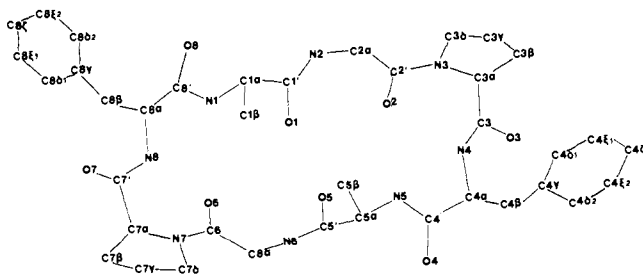


Figure 1. Atom numbering for *cyclo*(D-Ala-Gly-L-Pro-D-Phe)<sub>2</sub>.

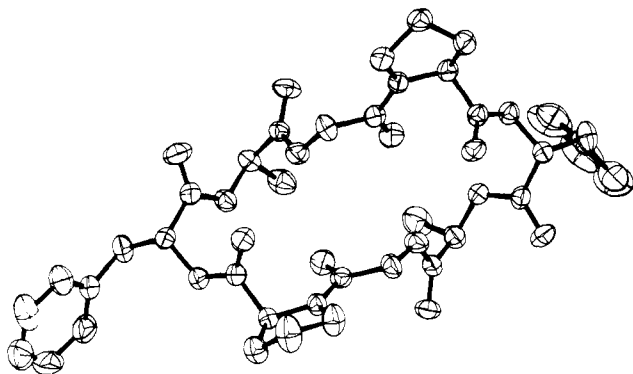


Figure 2. Crystal structure conformation of *cyclo*(D-Ala-Gly-L-Pro-D-Phe)<sub>2</sub>.

conformational energies were excluded, and accessible areas for N-H protons were calculated for the remainder.

A model of *cyclo*(D-Ala-Gly-L-Pro-D-Phe)<sub>2</sub> with dihedral angles closer to the NMR estimate was obtained by using the utilities of CHEMLAB and the Allinger MM1 program (QCPE 400).<sup>7</sup> A cyclic octapeptide of C<sub>2</sub> symmetry was obtained by joining at the Ala-Gly peptide bonds two Gly-L-Pro-D-Phe-D-Ala- units possessing the NMR-suggested dihedral angles and then locating a nearby conformational energy minimum, allowing only the positions of the glycine atoms to vary. The minimization was carried out by using MM1 with torsional and bending potential function parameters for the peptide backbone taken from Ramachandran and Sasisekharan.<sup>8</sup>

A model for *cyclo*(L-Ala-Gly-L-Pro-L-Phe)<sub>2</sub> was obtained beginning with the crystal structure of β-amanitin.<sup>3</sup> β-Amanitin has the backbone sequence Trp<sup>1</sup>-Gly<sup>2</sup>-Ile<sup>3</sup>-Gly<sup>4</sup>-Cys<sup>5</sup>-Asp<sup>6</sup>-Hypro<sup>7</sup>-diOHlle<sup>8</sup>. (The asterisks indicate oxidatively coupled side chains.) This backbone has a type II β-turn at L-Ile-Gly and a type I turn at Hypro-diOHlle. Retaining the positions of the backbone atoms in this structure, the side chains of Trp, Ile, Cys, and diOHlle were replaced by methyls, and the hydroxyl of Hypro and the side chain of Asp were replaced by hydrogen to give the sequence *cyclo*(Ala<sup>1</sup>-Gly<sup>2</sup>-Ala<sup>3</sup>-Gly<sup>4</sup>-Ala<sup>5</sup>-Gly<sup>6</sup>-Pro<sup>7</sup>-Phe<sup>8</sup>). The sequence of residues 5-6-7-8-1 in this model has backbone angles close to those proposed for *cyclo*(L-Ala-Gly-L-Pro-L-Phe)<sub>2</sub> in solution.<sup>1</sup> The Phe side chain of this model was rotated through the values of χ<sup>1</sup> and χ<sup>2</sup> indicated above to obtain structures for which N-H surface areas were calculated.

## Results

**Crystal Structure.** Figure 1 shows the numbering scheme used for *cyclo*(D-Ala-Gly-L-Pro-D-Phe)<sub>2</sub>. Table I lists the final atomic parameters, and Tables IIa,b lists the bond lengths and bond angles of the peptide. These agree with values reported for other peptides.<sup>9</sup> The average esd in bond lengths and angles are 0.004 Å and 0.3°.

The conformation of *cyclo*(D-Ala-Gly-L-Pro-D-Phe)<sub>2</sub> is shown in Figure 2, and the observed torsional angles are listed in Table III. The backbone shows approximate C<sub>2</sub> symmetry, although differences of up to 18° are observed in corresponding angles of

Table I. Positional Parameters and Their Estimated Standard Deviations for *cyclo*(D-Ala-Gly-L-Pro-D-Phe)<sub>2</sub>·2H<sub>2</sub>O·CH<sub>3</sub>OH

atom	X	Y	Z	B, Å <sup>2</sup>
N1	-0.1082 (3)	-0.567	0.1930 (3)	3.8 (1)
C1α	-0.0401 (4)	-0.5278 (4)	0.1625 (4)	3.7 (1)
C1β	0.0869 (5)	-0.4802 (6)	0.2764 (4)	5.1 (2)
C1'	-0.1132 (3)	-0.4426 (4)	0.0666 (3)	3.3 (1)
O1	-0.0962 (3)	-0.4294 (3)	0.0002 (3)	4.59 (9)
N2	-0.1926 (4)	-0.3823 (4)	0.0604 (3)	4.2 (1)
C2α	-0.2663 (4)	-0.2994 (4)	-0.0287 (4)	4.2 (1)
C2'	-0.1828 (4)	-0.2055 (4)	0.0005 (4)	3.4 (1)
O2	-0.0752 (3)	-0.1907 (3)	0.0996 (3)	4.4 (1)
N3	-0.2361 (3)	-0.1385 (3)	-0.0899 (3)	3.2 (1)
C3α	-0.1720 (4)	-0.0374 (4)	-0.0723 (4)	3.5 (1)
C3β	-0.2813 (4)	0.0255 (4)	-0.1867 (4)	4.2 (1)
C3γ	-0.3686 (5)	-0.0597 (5)	-0.2809 (4)	4.6 (2)
C3δ	-0.3655 (4)	-0.1472 (4)	-0.2102 (4)	3.9 (1)
C3'	0.8774 (4)	0.0204 (4)	0.0384 (3)	3.4 (1)
O3	-0.1861 (3)	0.0270 (3)	0.0639 (3)	4.30 (9)
N4	-0.0094 (3)	0.0683 (3)	0.1030 (3)	3.6 (1)
C4α	0.0361 (4)	0.1368 (4)	0.2011 (4)	3.6 (1)
C4β	0.1391 (4)	0.2145 (5)	0.2362 (5)	4.6 (2)
C4γ	0.2749 (4)	0.1763 (5)	0.3283 (4)	4.4 (1)
C4δ <sub>1</sub>	0.3624 (6)	0.2243 (7)	0.4406 (6)	7.0 (2)
C4ε <sub>1</sub>	0.4882 (7)	0.199 (1)	0.5233 (6)	8.9 (3)
C4ξ	0.5248 (7)	0.1191 (9)	0.4948 (6)	9.8 (3)
C4ε <sub>2</sub>	0.4420 (6)	0.0603 (9)	0.3852 (6)	8.3 (3)
C4δ <sub>2</sub>	0.3146 (5)	0.0955 (6)	0.3021 (5)	5.8 (2)
C4'	0.0828 (4)	0.0757 (4)	0.3097 (4)	3.6 (1)
O4	0.1013 (3)	0.1238 (3)	0.3894 (3)	4.8 (1)
N5	0.1061 (3)	-0.0285 (3)	0.3153 (3)	3.8 (1)
C5α	0.1481 (4)	-0.0908 (4)	0.4174 (4)	4.0 (1)
C5β	0.2127 (6)	-0.1934 (6)	0.4274 (5)	6.6 (2)
C5'	0.0387 (4)	-0.1189 (4)	0.4032 (4)	3.7 (1)
O5	0.0571 (3)	-0.1339 (3)	0.4933 (3)	4.41 (9)
N6	-0.0761 (4)	-0.1296 (4)	0.2931 (3)	4.4 (1)
C6α	-0.1859 (4)	-0.1634 (4)	0.2697 (4)	4.3 (1)
C6'	-0.1793 (4)	-0.2827 (4)	0.2932 (3)	3.3 (1)
O6	-0.0999 (3)	-0.3432 (3)	0.3124 (3)	4.6 (1)
N7	-0.2688 (3)	-0.3183 (3)	0.2872 (3)	3.5 (1)
C7α	-0.2721 (4)	-0.4306 (4)	0.3097 (3)	3.5 (1)
C7β	-0.3851 (4)	-0.4327 (5)	0.2989 (4)	4.5 (1)
C7γ	-0.4654 (5)	-0.3384 (6)	0.2242 (6)	7.6 (2)
C7δ	-0.3750 (5)	-0.2557 (5)	0.2539 (5)	5.2 (2)
C7'	-0.2995 (4)	-0.4996 (4)	0.2132 (3)	3.2 (1)
O7	-0.3660 (3)	-0.4679 (3)	0.1116 (3)	4.3 (1)
N8	-0.2492 (3)	-0.5975 (3)	0.2480 (3)	3.4 (1)
C8α	-0.2721 (4)	-0.6691 (4)	0.1612 (4)	3.6 (1)
C8β	-0.2143 (4)	-0.7797 (4)	0.2128 (4)	4.4 (1)
C8γ	-0.2738 (4)	-0.8426 (4)	0.2464 (4)	3.8 (1)
C8δ <sub>1</sub>	-0.3956 (5)	-0.8802 (5)	0.1601 (5)	4.9 (2)
C8ε <sub>1</sub>	-0.4487 (6)	-0.9454 (6)	0.1845 (6)	7.1 (2)
C8ξ	-0.3799 (6)	-0.9731 (6)	0.3018 (5)	8.5 (2)
C8ε <sub>2</sub>	-0.2572 (7)	-0.9369 (6)	0.3899 (5)	9.9 (2)
C8δ <sub>2</sub>	-0.2027 (7)	-0.8703 (5)	0.3623 (5)	6.3 (2)
C8'	-0.2148 (4)	-0.6244 (4)	0.1154 (4)	3.7 (1)
O8	-0.2639 (4)	-0.6443 (4)	0.0137 (3)	6.5 (1)
OW <sub>1</sub>	0.4007 (3)	0.4130 (4)	0.0156 (3)	5.4 (1)
OW <sub>2</sub>	0.0952 (4)	0.3373 (4)	0.4488 (3)	6.7 (2)
OMe	0.6987 (7)	0.3182 (9)	0.8170 (6)	13.8 (3)
CMe	0.8216 (8)	0.3091 (9)	0.8580 (7)	8.8 (3)

the main chain in the two Ala-Gly-Pro-Phe halves. All peptide links are trans, with ω deviating from 180° by no more than 8°. The backbone consists of two planes formed by the α-carbons of Ala-Gly-Pro-Phe-Ala sequences joined at an angle of 94° along a line between the ala α-carbons. The Ala methyl groups are directed toward each other on the convex side of the fold. There are two approximate type II β-turns formed by the L-Pro-D-Phe sequences, and these are followed by approximate type III' turns comprising the D-Phe-D-Ala pairs. The carbonyls of the Pro residues are directed into the concave side of the ring fold, and the Gly carbonyls point to the interior of the ring. There are no good intramolecular N-H...O hydrogen bonds, as is seen from the data of Table IV, although there are possible long distance (3.1-3.4 Å) bifurcated interactions of the Ala and Gly N-H units with their preceding Gly and Pro C=O groups.

(7) Allinger, N. L.; Yuh, Y. MM1 Molecular Mechanics Program, program No. 400, Quantum Chemistry Program Exchange, Department of Chemistry, Indiana University, Bloomington, IN 47405, 1975.

(8) Ramachandran, G. N.; Sasisekharan, V. *Adv. Protein Chem.* **1968**, *23*, 284-437.

(9) Benedetti, E. In "Peptides", Proceedings of the 5th American Peptide Symposium; Goodman, M., Meienhofer, J., Eds.; Wiley: New York, 1977; pp 257-273.

Table II. Bond Lengths<sup>a</sup> (Å) and Bond Angles<sup>b</sup> (deg) for *cyclo*(D-Ala-Gly-L-Pro-D-Phe)<sub>2</sub>

	D-Ala <i>i</i> = 1	Gly <i>i</i> = 2	L-Pro <i>i</i> = 3	D-Phe <i>i</i> = 4	D-Ala <i>i</i> = 5	Gly <i>i</i> = 6	L-Pro <i>i</i> = 7	D-Phe <i>i</i> = 8
(a) Bond Lengths								
Ni-Ci $\alpha$	1.462	1.451	1.489	1.457	1.476	1.445	1.465	1.462
Ci $\alpha$ -C'i	1.521	1.525	1.520	1.529	1.500	1.532	1.535	1.540
C'i-Oi	1.237	1.235	1.244	1.235	1.251	1.240	1.218	1.233
C'i-N( <i>i</i> +1)	1.338	1.337	1.343	1.342	1.336	1.327	1.341	1.342
Ci $\alpha$ -Ci $\beta$	1.544		1.553	1.542	1.544		1.544	1.536
Ci $\beta$ -Ci $\gamma$			1.528				1.499	
Ci $\gamma$ -Ci $\delta$			1.539				1.482	
Ci $\delta$ -Ni			1.479				1.477	
Ci $\beta$ -Ci $\gamma$				1.510				1.518
Ci $\gamma$ -Ci $\delta$ <sub>1</sub>				1.401				1.371
Ci $\delta$ <sub>1</sub> -Ci $\epsilon$ <sub>1</sub>				1.362				1.357
Ci $\epsilon$ <sub>1</sub> -Ci $\zeta$				1.355				1.390
Ci $\zeta$ -Ci $\epsilon$ <sub>2</sub>				1.438				1.376
Ci $\epsilon$ <sub>2</sub> -Ci $\delta$ <sub>2</sub>				1.413				1.417
Ci $\delta$ <sub>2</sub> -Ci $\gamma$				1.369				1.367
(b) Bond Angles								
C'(i-1)-Ni-Ci $\alpha$	121.2	120.4	120.9	118.6	119.0	122.5	120.3	118.8
Ci $\alpha$ -Ni-Ci $\delta$			112.6				113.3	
C'(i-1)-Ni-C $\delta$			126.1				126.3	
C'i-Ci $\alpha$ -Ni	112.9	111.3	111.1	113.4	111.6	110.8	109.8	111.2
Ni-Ci $\alpha$ -Ci $\beta$	107.7		102.1	111.6	108.6		101.6	112.6
Ci $\beta$ -Ci $\alpha$ -C'i	108.8		111.3	110.7	109.6		110.9	107.2
Ci $\alpha$ -C'i-Oi	120.6	123.4	121.8	119.5	119.8	123.5	121.6	120.6
N( <i>i</i> +1)-C'i-Ci $\alpha$	116.9	114.5	115.6	117.4	118.1	114.8	115.2	116.3
N( <i>i</i> +1)-C'i-Oi	122.5	122.1	122.5	123.1	122.1	121.7	123.1	123.1
Ci $\alpha$ -Ci $\beta$ -Ci $\gamma$			104.8				105.8	
Ci $\beta$ -Ci $\gamma$ -Ci $\delta$			102.8				105.4	
Ci $\gamma$ -Ci $\delta$ -Ni			103.4				103.2	
Ci $\alpha$ -Ci $\beta$ -Ci $\gamma$				116.9				114.5
Ci $\beta$ -Ci $\gamma$ -Ci $\delta$ <sub>1</sub>				120.6				120.4
Ci $\beta$ -Ci $\gamma$ -Ci $\delta$ <sub>2</sub>				120.2				120.1
Ci $\delta$ <sub>2</sub> -Ci $\gamma$ -Ci $\delta$ <sub>1</sub>				119.2				119.3
Ci $\gamma$ -Ci $\delta$ <sub>1</sub> -Ci $\epsilon$ <sub>1</sub>				123.0				122.6
Ci $\delta$ <sub>1</sub> -Ci $\epsilon$ <sub>1</sub> -Ci $\zeta$				116.3				119.5
Ci $\epsilon$ <sub>1</sub> -Ci $\zeta$ -Ci $\epsilon$ <sub>2</sub>				125.3				118.9

<sup>a</sup> Average esd for bond lengths is 0.004 Å. <sup>b</sup> Average esd for bond angles is 0.3°.

Table III. Conformational Angles (deg) for Crystalline *cyclo*(D-Ala-Gly-L-Pro-D-Phe)<sub>2</sub>

angle <sup>a</sup>	D-Ala 1	Gly 2	L-Pro 3	D-Phe 4	D-Ala 5	Gly 6	L-Pro 7	D-Phe 8
$\phi$	68	-72	-47	74	79	-74	-65	63
$\psi$	29	165	142	16	29	173	150	33
$\omega$	-180	174	172	-179	176	-179	179	175
$\chi^0$			9				-5	
$\chi^1$			-29	-89			23	66
$\chi^2$			38	-114			-33	117
$\chi^3$			-32	4			29	-1
$\chi^4$			15	-4			-15	2
$\chi^5$				0				-3
$\chi^6$				3				2
$\chi^7$				-3				0
$\chi^8$				-1				0

<sup>a</sup> Main chain:  $\phi$ , C'(i-1)-Ni-Ci $\alpha$ -C'i;  $\psi$ , Ni-Ci $\alpha$ -C'i-N(i+1);  $\omega$ , Ci $\alpha$ -C'i-N(i+1)-C(i+1) $\alpha$ . Pro:  $\chi^0$ , Ci $\delta$ -Ni-Ci $\alpha$ -Ci $\beta$ ;  $\chi^1$ , Ni-Ci $\alpha$ -Ci $\beta$ -Ci $\gamma$ ;  $\chi^2$ , Ci $\alpha$ -Ci $\beta$ -Ci $\gamma$ -Ci $\delta$ ;  $\chi^3$ , Ci $\beta$ -Ci $\gamma$ -Ci $\delta$ -Ni;  $\chi^4$ , Ci $\gamma$ -Ci $\delta$ -Ni-Ci $\alpha$ . Phe:  $\chi^1$ , Ni-Ci $\alpha$ -Ci $\beta$ -Ci $\gamma$ ;  $\chi^2$ , Ci $\alpha$ -Ci $\beta$ -Ci $\gamma$ -Ci $\delta$ <sub>1</sub>;  $\chi^3$ , Ci $\delta$ <sub>2</sub>-Ci $\gamma$ -Ci $\delta$ <sub>1</sub>-Ci $\epsilon$ <sub>1</sub>;  $\chi^4$ , Ci $\gamma$ -Ci $\delta$ <sub>1</sub>-Ci $\epsilon$ <sub>1</sub>-Ci $\zeta$ ;  $\chi^5$ , Ci $\delta$ <sub>1</sub>-Ci $\epsilon$ <sub>1</sub>-Ci $\zeta$ -Ci $\epsilon$ <sub>2</sub>;  $\chi^6$ , Ci $\epsilon$ <sub>1</sub>-Ci $\zeta$ -Ci $\epsilon$ <sub>2</sub>-Ci $\delta$ <sub>2</sub>;  $\chi^7$ , Ci $\zeta$ -Ci $\epsilon$ <sub>2</sub>-Ci $\delta$ <sub>2</sub>-Ci $\gamma$ ;  $\chi^8$ , Ci $\epsilon$ <sub>2</sub>-Ci $\delta$ <sub>2</sub>-Ci $\gamma$ -Ci $\delta$ <sub>1</sub>.

In the crystal the two Phe side chains have different rotameric states.  $\chi^1$  of D-Phe<sup>4</sup> is -89° and  $\chi^1$  of D-Phe<sup>8</sup> is 65°. The two proline rings also differ: Pro<sup>3</sup> has C $\gamma$  endo and Pro<sup>7</sup> has C $\gamma$  exo.

The crystal packing as viewed down the crystallographic *b* axis is shown in Figure 3. As in other cases,<sup>10,11</sup> the hydrophobic

Table IV. Potential Hydrogen Bond Interactions (Å) in *cyclo*(D-Ala-Gly-L-Pro-D-Phe)<sub>2</sub>

atom 1	atom 2	symmetry <sup>a</sup>	distance (esd)
N1	O6	I (000)	3.339 (3)
N1	O7	I (000)	3.281 (3)
N1	OW2	I (0-10)	3.124 (3)
O1	N4	II (0-10)	2.914 (3)
N2	O6	I (000)	3.193 (3)
N2	O7	I (000)	3.329 (3)
N2	O8	I (000)	3.382 (3)
O2	N5	I (000)	3.186 (3)
O2	N6	I (000)	3.134 (3)
N3	OW1	II (0-10)	3.391 (3)
O3	N5	I (000)	3.297 (3)
O3	N6	I (000)	3.363 (3)
O3	OW1	II (0-10)	2.838 (3)
O4	OW2	I (000)	2.865 (3)
O5	N8	II (001)	2.946 (2)
O7	OW1	I (-1-10)	3.009 (3)
O8	OMe	I (-1-1-1)	2.768 (5)

<sup>a</sup>Symmetry: I, *x,y,z*; II,  $-x, 1/2+y, -z$ .

regions of the peptides tend to segregate.

**Comparison of Crystal and Solution Conformations.** In the crystal the backbone of the D-Ala, D-Phe peptide is similar but not identical with one of the two conformations proposed as probable on the basis of solution NMR measurements. When average values of the backbone torsional angles in the crystal are compared with the backbone angles of this proposed solution conformation, agreement is good except for 25° deviations at  $\phi_{\text{Phe}}$  and  $\phi_{\text{Ala}}$  and a 45° deviation at  $\psi_{\text{Phe}}$  (Table V). These differences correspond to a change that is primarily visible as a rotation of the plane of the Phe-Ala peptide link. In the crystal conformation ( $\psi_{\text{Phe}} \approx +25^\circ$ ,  $\phi_{\text{Ala}} \approx 74^\circ$ ), the Ala N-H proton is more exposed

(10) Kartha, G.; Bhandary, K. K.; Koppale, K. D.; Go, A.; Zhu, P.-P. *J. Am. Chem. Soc.* **1984**, *106*, 3844-3850.

(11) Karle, I. L. In "Peptides", Proceedings of the 6th American Peptide Symposium; Gross, E., Meienhofer, J., Eds.; Pierce Chemical Co.: Rockford, IL, 1979; pp 681-690.

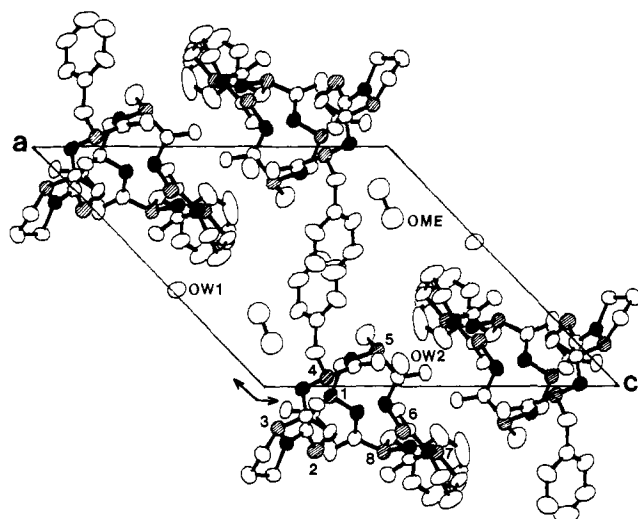


**Figure 3.** Packing of peptide and solvent molecules in the crystal of *cyclo*(D-Ala-Gly-L-Pro-D-Phe)<sub>2</sub>·2H<sub>2</sub>O·CH<sub>3</sub>OH viewed down the crystallographic *b* axis. The  $\alpha$ -carbon atoms (shaded) of one molecule are numbered. The solid circles represent nitrogens.

**Table V.** Main Chain Torsional Angles (deg) of *cyclo*(D-Ala-Gly-L-Pro-D-Phe)<sub>2</sub> in Solution and the Crystal

	D-Ala		Gly		L-Pro		D-Phe	
	$\phi$	$\psi$	$\phi$	$\psi$	$\phi$	$\psi$	$\phi$	$\psi$
crystal average	74	29	-73	169	-56	146	69	25
NMR estimate <sup>a</sup>	100	40	-80	180	-60	150	95	-20
C <sub>2</sub> model for surface calcn	100	40	-108	170	-64	150	95	-20

<sup>a</sup> Conformation B of ref 1. <sup>b</sup> All values of  $|\omega| > 170^\circ$ .

to solvent than it is in the NMR model ( $\psi_{\text{Phe}} \approx -20^\circ$ ,  $\phi_{\text{Ala}} \approx 100^\circ$ ). The difference between the two conformations is outside the uncertainty inherent in the NMR coupling constant—dihedral angle correlations. The average value of  $\phi_{\text{Ala}}$  near  $74^\circ$  found in the crystal corresponds to an H-N-C-H dihedral angle near  $134^\circ$  and an H-N-C-H coupling constant for Ala near 6 Hz. This is in significant disagreement with the observed 8.4-Hz value, which indicates a definitely larger (ca.  $160^\circ$ ) H-N-C-H angle.<sup>1,12,13</sup>

Another real difference between crystal and solution conformations is that the NMR evidence ( $H_\alpha$ - $H_\beta$  coupling constants and diamagnetic shielding of adjacent proline ring protons) indicates that in solution the Phe side chain is almost entirely in the rotamer state with  $\chi^1 = 60^\circ$ .<sup>1</sup> In the crystal  $66^\circ$  and  $-89^\circ$  occur.

**Exposure of N-H Protons.** Models of the crystal backbone and that derived from the NMR data suggest a difference between them in solvent exposure of the Ala N-H proton, although the extent of this difference cannot be estimated by visual inspection. (See Figure 4.) Therefore, we calculated the solvent exposure of N-H protons for the crystal conformation with different rotations of the Phe side chain, and for models with a backbone more closely approaching the estimated solution conformation. The solution model, of C<sub>2</sub> symmetry, was constructed to maintain  $\psi_{\text{Phe}}$  near  $-20^\circ$  instead of the  $+20^\circ$  found in the crystal. Its backbone dihedral angles are given as the third entry in Table V.

Calculated surface areas for conformations of models of the D-Ala, D-Phe peptide are given in Table VI. Results for representative rotations of  $\chi^1$  of the Phe side chain are given at  $\chi^2 = 90^\circ$ . Calculations were also made for  $\chi^2 = 0^\circ$ , but these conformations generally proved to have high steric energy, and are deemed unlikely. The areas shown are the areas of the van der Waals surface of the N-H protons that can come into contact

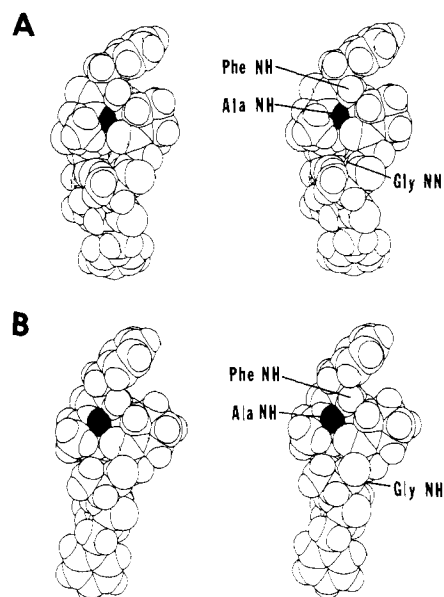


**Figure 4.** Space-filling representations of the NMR-based model (A) and the crystal structure (B) of *cyclo*(D-Ala-Gly-L-Pro-D-Phe)<sub>2</sub>. The Ala N-H, which differs in solvent exposure in the two conformations, is darkened.

**Table VI.** Exposed Surface Areas ( $\text{\AA}^2$ ) of N-H Protons for Several Conformations of *cyclo*(D-Ala-Gly-L-Pro-D-Phe)<sub>2</sub><sup>a</sup>

conformation <sup>b</sup>	Ala <sup>1</sup>	Gly <sup>2</sup>	Phe <sup>4</sup>	Ala <sup>5</sup>	Gly <sup>6</sup>	Phe <sup>8</sup>
crystal structure						
probe radius = 0 $\text{\AA}$	8.82	8.06	10.76	7.24	8.08	9.60
probe radius = 1.4 $\text{\AA}$	0.70	0.00	0.80	0.18	0.00	1.16
crystal structure with						
$\chi^1_8 = 60^\circ, \chi^2_8 = 90^\circ$	0.70				0.00	0.40
$\chi^1_8 = 180^\circ, \chi^2_8 = 90^\circ$	0.70				0.00	2.62
$\chi^1_8 = -60^\circ, \chi^2_8 = 90^\circ$	0.18				0.00	0.36
$\chi^1_4 = 60^\circ, \chi^2_4 = 90^\circ$		0.00	0.96	0.72		
$\chi^1_4 = 180^\circ, \chi^2_4 = 90^\circ$		0.00	2.62	0.72		
$\chi^1_4 = -60^\circ, \chi^2_4 = 90^\circ$		0.00	0.28	0.34		
C <sub>2</sub> solution model <sup>d</sup> with						
$\chi^1 = 60^\circ, \chi^2 = 90^\circ$ , probe = 0 $\text{\AA}$	9.82	10.48	6.44			
$\chi^1 = 60^\circ, \chi^2 = 90^\circ$ , probe = 1.4 $\text{\AA}$	0.01	1.78	0.00			
$\chi^1 = 180^\circ, \chi^2 = 90^\circ$	0.01	2.85	0.00			
$\chi^1 = 60^\circ, \chi^2 = 90^\circ$	0.01	0.61	0.00			
obsd $k_{\text{nitroxy}}$ , L mol <sup>-1</sup> s <sup>-1</sup>	100	450	110			
obsd $d\delta/dT$ , ppm/deg (upfield)	0.0003	0.0043	0.0012			

<sup>a</sup> Numbering corresponds to Figure 1. <sup>b</sup> Departures from the crystal structure are given. For clarity, areas are given only for the atoms in the half-molecule containing the rotated side chain. <sup>c</sup>  $\chi^1 = 60^\circ$  corresponds to NMR solution estimate. <sup>d</sup> Backbone dihedral angles of third entry in Table V. Since this is a C<sub>2</sub> structure,  $\chi^1$  and  $\chi^2$  are for the single Phe type present.

with a 1.4- $\text{\AA}$  probe sphere. For the crystal structure and the model of the most likely solution conformation, the total van der Waals surfaces (probe radius = 0) are also given.

In both the crystal and solution models the Gly N-H protons are fully sequestered by the peptide backbone. They show no area accessible to a 1.4- $\text{\AA}$  sphere. As expected, Phe N-H exposure is reduced when Phe side chain rotation  $\chi^1$  is near  $60^\circ$  or  $-60^\circ$ . The reduction is greater at  $-60^\circ$ . However, exposure of the Ala N-H differs importantly in the two models. In models based on the crystal backbone, the Ala N-H presents some exposed surface, although it is more hidden when  $\chi^1_{\text{Phe}}$  is near  $-60^\circ$ . In contrast, it is fully buried to the 1.4- $\text{\AA}$  sphere in the models based on the proposed solution backbone. This difference in exposure is visible in the space-filling models compared in Figure 4.

For comparison of the exposed areas given in Table VI with measurements made on solutions, the models with  $\chi^1_{\text{Phe}}$  near  $+60^\circ$

(12) Ramachandran, G. N.; Chandrasekharan, R.; Kopple, K. D. *Biopolymers* **1971**, *10*, 2113-2131.

(13) DeMarco, A.; Llinas, M.; Wuthrich, K. *Biopolymers* **1978**, *17*, 637-650.

**Table VII.** Exposed Surface Areas ( $\text{\AA}^2$ ) of N-H Protons in a Model of *cyclo*(Ala<sup>1</sup>-Gly<sup>2</sup>-Ala<sup>3</sup>-Gly<sup>4</sup>-Ala<sup>5</sup>-Gly<sup>6</sup>-Pro<sup>7</sup>-Phe<sup>8</sup>) Based on the  $\beta$ -Amanitin Backbone<sup>a</sup>

Phe side chain angles (deg)	probe radius ( $\text{\AA}$ )	Ala <sup>1</sup>	Gly <sup>6</sup>	Phe <sup>8</sup>
$\chi^1 = 60, \chi^2 = 90$	1.4	0.00	0.00	0.00
$\chi^1 = 180, \chi^2 = 90$	1.4	0.04	0.00	0.82
	0	7.46	5.44	9.74
$\chi^1 = 60, \chi^2 = 0$	1.4	0.04	0.00	0.66
	0	7.46	5.44	9.74
$\chi^1 = 60, \chi^2 = 90$	1.4	0.04	0.00	0.12
	0	7.40	5.32	9.72
obsd $k_{\text{nitroxyl}}$ , L mol <sup>-1</sup> s <sup>-1</sup>		110	140	250
obsd $d\delta/dT$ , ppm/deg (upfield)		0.001	0.0026	0.003

<sup>a</sup>The backbone dihedral angles (deg) ( $\phi, \psi$ ) of the model are the following: (-110, -39),<sup>1</sup> (141, -178),<sup>2</sup> (-59, 126),<sup>3</sup> (88, -4),<sup>4</sup> (-122, -84),<sup>5</sup> (-175, 179),<sup>6</sup> (-60, -37),<sup>7</sup> (-80, -24).<sup>8</sup> All values of  $|\omega|$  are  $>170^\circ$ . <sup>b</sup> $\chi^1 = -60^\circ$  is the NMR solution estimate of the predominant rotamer.

should be used, since the NMR data indicate that this rotamer is almost exclusively favored. For  $\chi^1 = +60^\circ$ , the crystal backbone model indicates a similar degree of exposure to solvent for the Ala and Phe N-H, but no exposure of the Gly N-H. On the other hand, the solution backbone model has the Phe N-H exposed but both Ala and Gly N-H fully hidden, regardless of the position of the Phe side chain. At the bottom of Table VI are given the nitroxyl-catalyzed relaxation rates observed earlier<sup>1</sup> for the N-H protons of *cyclo*(D-Ala-Gly-L-Pro-D-Phe)<sub>2</sub> in dimethyl sulfoxide. The observation is that the Gly and Ala constants are similar and relatively small and the Phe rate constant is considerably higher. The solution backbone model is consistent with observation, but the crystal model is not. Thus the existence of the suggested difference between the proposed solution conformation and the crystal conformation, for which the primary argument was based on coupling constant data, is supported, semiquantitatively, by a correlation between the observed nitroxyl-catalyzed relaxation rates and the surface area estimates for the proposed solution conformation.

It must be emphasized that for the means employed above to distinguish among conformation choices to be quantitatively valid, the peptide studied must exist in solution in a single conformation. Evidence that *cyclo*(D-Ala-Gly-L-Pro-D-Phe)<sub>2</sub> probably does occupy a small region of conformation space in dimethyl sulfoxide was presented in the previous paper.<sup>1</sup>

Table VI also shows that the exposed surface area of the N-H protons in the solution model also parallels the previously observed<sup>1</sup> temperature dependence of chemical shift for these protons. However, solvent exposure may be only one component of these coefficients, and it would be risky to assume even a semiquantitative correlation.

***cyclo*(L-Ala-Gly-L-Pro-L-Phe)<sub>2</sub>.** The solution conformation of *cyclo*(L-Ala-Gly-L-Pro-L-Phe)<sub>2</sub>, like that of the D-Ala, D-Phe diastereomer, also appears to be well defined and it can be modeled by half of the backbone of crystalline  $\beta$ -amanitin.<sup>1,3</sup> Therefore it was of interest to compare calculated N-H surface areas with observed<sup>1</sup> nitroxyl rates and temperature coefficients for this L-Ala, L-Phe peptide. Construction of the model is described in the Experimental Section. Results are presented in Table VII. Bad contacts exclude  $\chi^1 = 60$  and  $180^\circ$  when  $\chi^2$  is  $0^\circ$ . The solution NMR data indicate that  $\chi^1 = -60^\circ$  almost entirely.<sup>1</sup>

The  $\beta$ -turn involved in this structure (L-Pro-L-Phe) is of type I. Visual inspection of space-filling models shows that in type I turns generally the N-H of the  $i + 2$  residue is more shielded from the environment by the side chains of the flanking residues than in type II turns. In agreement, the calculations shows the Phe N-H in this case to present significantly less surface to the 1.4- $\text{\AA}$  probe sphere, even when the Phe side chain is directed away from the Pro-Phe peptide bond ( $\chi^1 = 180^\circ$ ). There is agreement between N-H exposure and nitroxyl relaxation rate constants, in that the Ala and Gly N-H's are again sequestered and have lower constants, close to those for Ala and Gly in *cyclo*(D-Ala-Gly-L-Pro-D-Phe)<sub>2</sub>, while the Phe N-H is more exposed and has a higher rate constant, but one not so high as in the L-Pro-D-Phe

turn of the D-Ala, D-Phe peptide, where the exposed surface is greater.

## Conclusions

**Conformation of *cyclo*(D-Ala-Gly-L-Pro-D-Phe)<sub>2</sub>.** The crystal structures of *cyclo*(D-Ala-Gly-L-Pro-D-Phe) and of  $\beta$ -amanitin<sup>3</sup> and the NMR results for solution in dimethyl sulfoxide reported earlier<sup>1</sup> reinforce each other in indicating that the backbone conformation consisting of two approximately planar  $\beta$ -structures joined at an angle along a line between C <sub>$\alpha$</sub> <sup>1</sup> and C <sub>$\alpha$</sub> <sup>5</sup> is a readily attainable stable form for cyclic octapeptides.

The difference between solution and crystal conformations for the backbone of the D-Ala, D-Phe peptide is largely a matter of peptide bond plane rotation, in which the plane of the D-Phe-D-Ala CONH unit rotates about  $30^\circ$  relative to the average plane of the Ala-Gly-Pro-Phe-Ala  $\alpha$ -carbons. No specific single interaction in the crystal or in solution appears to account for the difference, however. This form of mobility in cyclic peptides probably has a low barrier, since the torsional barriers about  $\phi$  and  $\psi$  are low, and since rotation of the planes containing trans peptide bonds can occur in many cases without major changes in the rest of the backbone geometry. Hydrogen bonding involving the rotated peptide link would, of course, be affected. In a related case, preliminary reports have appeared of two crystal structures of another peptide in this series, *cyclo*(D-Ala-Gly-L-Pro-L-Phe)<sub>2</sub>, which differ in just this fashion.<sup>14,15</sup> There is a C<sub>2</sub> structure containing type I L-Pro-L-Phe  $\beta$ -turns which is analogous to the backbones described for the D-Ala, D-Phe and L-Ala, L-Phe cyclic octapeptides, and there has also been found a second, unsymmetrical structure with a backbone that differs very much from the first except for an almost  $180^\circ$  rotation of one Ala-Gly CONH plane relative to the local peptide ring plane.

**Correlation of Exposed Surface and Nitroxyl-Catalyzed Relaxation.** We have demonstrated here that nitroxyl-catalyzed relaxation can be used as a semiquantitative measure of exposed surface area in two cases where the backbone conformation in solution is probably stable and in which possible changes in exposure arising from side chain conformation do not introduce ambiguity. There are undoubtedly other cyclic peptides for which such treatment is possible. However, there are obvious limitations to quantitative interpretation of nitroxyl rates when there is conformational mobility in solution. With truly rigid molecules it would be possible to determine how nitroxyl-catalyzed relaxation depends on exposure to solvent. In the present work we used a water-sized probe ( $r = 1.4 \text{ \AA}$ ), but it is not obvious that this is the proper probe size. It may also be, since the relaxation occurs by a dipole-dipole interaction and is dependent on  $\langle r^{-6} \rangle$ , that a better correlation might be with the distance of closest possible approach for the free radical, rather than with the amount of exposed surface.

**Acknowledgment.** The X-ray crystallographic work was supported by a Grant from the National Institutes of Health, GM 22490, and by the New York State Department of Health. The calculations of surface area were supported by NIH Grant GM 26071 and were made on the IIT Chemistry Department VAX 11/750, which was funded in part by grants from the National Science Foundation (CHE 8306272) and the Camille and Henry Dreyfus Foundation.

**Registry No.** *cyclo*(D-Ala-Gly-L-Pro-D-Phe)<sub>2</sub>, 91302-75-9; *cyclo*(L-Ala-Gly-L-Pro-L-Phe)<sub>2</sub>, 91383-23-2; *cyclo*(Ala-Gly-Ala-Gly-Ala-Gly-Pro-Phe), 96928-69-7.

**Supplementary Material Available:** Table of observed and calculated structure factors for *cyclo*(D-Ala-Gly-L-Pro-D-Phe)<sub>2</sub>·2H<sub>2</sub>O·CH<sub>3</sub>OH (22 pages). Ordering information is given on any current masthead page.

(14) Bhandary, K.; Kartha, G.; Kopple, K. D. *Abstracts, Am. Cryst. Assoc. Meeting 1983, Aug. 1-5*, PD14, p 32.

(15) Bhandary, K. K.; Kartha, G.; Kopple, K. D. *Abstracts, Am. Cryst. Assoc. Meeting 1984, May 20-25*, PC13, p 53.